forests

MDPI

Article

A Hybrid Landslide Warning Model Coupling Susceptibility Zoning and Precipitation

Deliang Sun [1], Qingyu Gu [1], Haijia Wen [2,*], Shuxian Shi [3], Changlin Mi [4] and Fengtai Zhang [5]

[1] Key Laboratory of GIS Application Research, Chongqing Normal University, Chongqing 401331, China; 20130831@cqnu.edu.cn (D.S.); guqingy00@gmail.com (Q.G.)
[2] Key Laboratory of New Technology for Construction of Cities in Mountain Area, Ministry of Education, Chongqing University, Chongqing 400045, China
[3] Key Laboratory of Geographic Information Science, Ministry of Education, East China Normal University, Shanghai 200241, China; shelly-shi@outlook.com
[4] Natural Resources Development Service Center of Linyi, Linyi 276000, China; michanglin@ly.shandong.cn
[5] School of Management, Chongqing Technology and Business University, Chongqing 400054, China; zhfthero45@cqut.edu.cn
* Correspondence: jhw@cqu.edu.cn

Abstract: Landslides are one of the most severe and common geological hazards in the world. The purpose of this research is to establish a coupled landslide warning model based on random forest susceptibility zoning and precipitation. The 1520 landslide events in Fengjie County, Chongqing, China, before 2016 are taken as research cases. We adapt the random forest model to build a landslide susceptibility model. The antecedent effective precipitation model, based on the fractal relationship, is used to calculate the antecedent effective precipitation in the 10 days before the landslide event. Based on different susceptibility zones, the effective precipitation corresponding to different cumulative frequencies is counted as the threshold, and the threshold is adjusted according to the fitted curve. Finally, according to the daily precipitation, the rain warning levels in susceptibility zones are further adjusted, and the final prewarning model of the susceptibility zoning and precipitation coupling is obtained. The results show that the random forest model has good prediction ability for landslide susceptibility zoning, and the precipitation warning model that couples landslide susceptibility, antecedent effective precipitation, and the daily precipitation threshold has high early warning ability. At the same time, it was found that the precipitation warning model coupled with antecedent effective precipitation and the daily precipitation threshold has more accurate precipitation warning ability than the precipitation warning model coupled with the antecedent effective precipitation only; the coupling of the two can complement each other to better characterize the occurrence of landslides triggered by rainfall. The proposed coupled landslide early warning model based on random forest susceptibility and rainfall inducing factors can provide scientific guidance for landslide early warning and prediction, and improve the manageability of landslide risk.

Keywords: landslide susceptibility; antecedent effective precipitation; daily precipitation; hybrid landslide warning model

check for updates

Citation: Sun, D.; Gu, Q.; Wen, H.; Shi, S.; Mi, C.; Zhang, F. A Hybrid Landslide Warning Model Coupling Susceptibility Zoning and Precipitation. *Forests* **2022**, *13*, 827. https://doi.org/10.3390/f13060827

Academic Editor: Filippo Giadrossich

Received: 27 March 2022
Accepted: 23 May 2022
Published: 25 May 2022

Publisher's Note: MDPI stays neutral with regard to jurisdictional claims in published maps and institutional affiliations.

Copyright: © 2022 by the authors. Licensee MDPI, Basel, Switzerland. This article is an open access article distributed under the terms and conditions of the Creative Commons Attribution (CC BY) license (https://creativecommons.org/licenses/by/4.0/).

1. Introduction

A landslide is a geological disaster with further impact, and threatens the safety and property of human life to a certain extent [1]. According to the China Statistical Yearbook, from 2000 to 2019, a total of 320,000 natural disasters occurred, causing a total economic loss of 9.894 billion dollars. Of these, 220,000 landslide disasters occurred, accounting for 70.2% of the total. Chongqing is one of the four major geological disaster areas in China. Geological disasters cause about 40–60 deaths and direct economic losses of about 300–400 million yuan per year, accounting for more than 20% of the city's natural disaster losses. Among them, the Longjing landslide in Shizhu County, Chongqing, had a scale

of about 142.83 × 104 m^3, directly threatening 2864 residents and 1630 pupils in primary schools, as well as roads, pipelines, and other urban infrastructure. According to the World Health Organization (WHO) report, between 1998 and 2017, the population affected by landslides was 4.8 million, and they caused more than 18,000 deaths. The main impacts of landslides include the destruction of houses and roads, damage to water storage facilities, and the blockage of rivers, causing huge casualties and economic losses [2]. Therefore, it is necessary to conduct a geological disaster investigation and an assessment of potential landslide occurrence areas, and take corresponding preventive measures to reduce the economic losses and casualties caused by landslides.

Landslide susceptibility is an effective method to prevent landslide disasters. It is based on local geological environment factors to evaluate the spatial distribution of landslide occurrence probability in specific areas; it is also an important means to study the occurrence of landslides [3]. The evaluation of landslide susceptibility began in the mid-1970s. Carrara [4] used a large number of data on landslides, topography, landforms, field surveys, etc., based on expert experience and other methods, to evaluate landslide susceptibility in the Columbia area. Many scholars divide landslide susceptibility modeling methods into two categories, qualitative and quantitative. Qualitative methods use prior knowledge to assess the occurrence of landslides [5,6]. This method is based on expert experience, and has the disadvantage of being subjective, which makes the differences between the models more significant. Quantitative methods use mathematical–statistical models to evaluate landslides [7–9]. The accuracy and completeness of the input landslide data have a greater impact on the statistical model. This model has higher requirements for data collection. With the development of GIS and machine learning, many scholars use machine learning methods to conduct landslide susceptibility evaluation studies in different research areas [10–14]. Sun et al. (2020) used an optimized random forest model to establish a landslide susceptibility model in Fengjie County, Chongqing City, and applied the model to Wushan County, Chongqing City, to discuss the generalization ability of the model based on random forest. The results show that the model had high susceptibility simulation ability and a good generalization effect [15]. At the same time, they compared the accuracy of different machine learning methods. Many scholars chose multiple machine learning algorithms—for example, logical model trees, random forest, classification regression trees, XGBoost, etc.—to build a landslide susceptibility model. Moayedi et al. used the artificial neural network model optimized by particle swarm to predict the landslide susceptibility in the Layleh valley area, and achieved good prediction results [16]. Pourghasemi et al. used 10 machine learning algorithms, such as artificial neural network (ANN), boosted regression trees (BRT), and random forest (RF), to model landslide susceptibility in the Ghaemshahr region of Iran, and found that RF (AUC = 83.7%) had the best prediction performance [17]. Zhou et al. developed a novel interpretable model based on SHAP and XGBoost, which provided 0.75 accuracy and 0.83 AUC value for the test sets [18]. Research has shown that the predictive ability of the random forest model is more significant in general [19–22].

Rainfall is the most important factor inducing landslides. At present, there are two main rainfall threshold models, a physical rainfall threshold and an empirical rainfall threshold [23–25]; the empirical threshold is based on the relationship between a large number of landslides and rainfall data, and is currently the most commonly used rainfall threshold model. Rainfall intensity and accumulation are the two main aspects that affect the rainfall threshold. There are many studies on this [26–28]. At present, there are two main types of precipitation threshold statistical models for studying landslides at home and abroad: daily precipitation [29] and antecedent effective precipitation [30,31]. However, research on the impact of precipitation on landslides is lagging [32,33], and threshold research cannot be conducted solely from the daily precipitation or antecedent effective precipitation accumulation. Therefore, it is necessary to adjust the existing precipitation threshold model according to the situation of the study area.

The occurrence of landslides is the result of the combined effects of natural conditions and human activities, in which rainfall triggers the occurrence of landslides. In high-susceptibility areas, relatively low precipitation can trigger the occurrence of landslides. The occurrence of landslides is related to the susceptibility of the area where the landslide is located, and also to the precipitation in the area. The study of landslide-inducing factors mainly considers the daily precipitation or the antecedent effective precipitation. There are few studies based on the susceptibility of landslides that consider multiple precipitation-inducing factors [34,35]. In this paper, the random forest model is used to evaluate the susceptible zones in the study area, and a landslide space–time joint early warning and forecast model is constructed according to the antecedent effective precipitation and the daily precipitation.

2. Materials and Methods

2.1. Methodology

Based on 16 evaluation factors and the random forest model, the landslide susceptibility zoning was established. Subsequently, based on the previous effective rainfall and the rainfall on the day of the landslide, rainfall-induced landslide early warning and forecasting was carried out. Based on the rainfall in the first 10 days of the landslide, the attenuation coefficient of the rainfall in the early stage of the landslide was calculated, and the threshold of the effective rainfall in the early stage of the landslide was constructed according to the frequency of landslide occurrence in each susceptibility zone. At the same time, the landslide warning and forecasting model was adjusted based on the rainfall that day. The specific steps are shown in Figure 1.

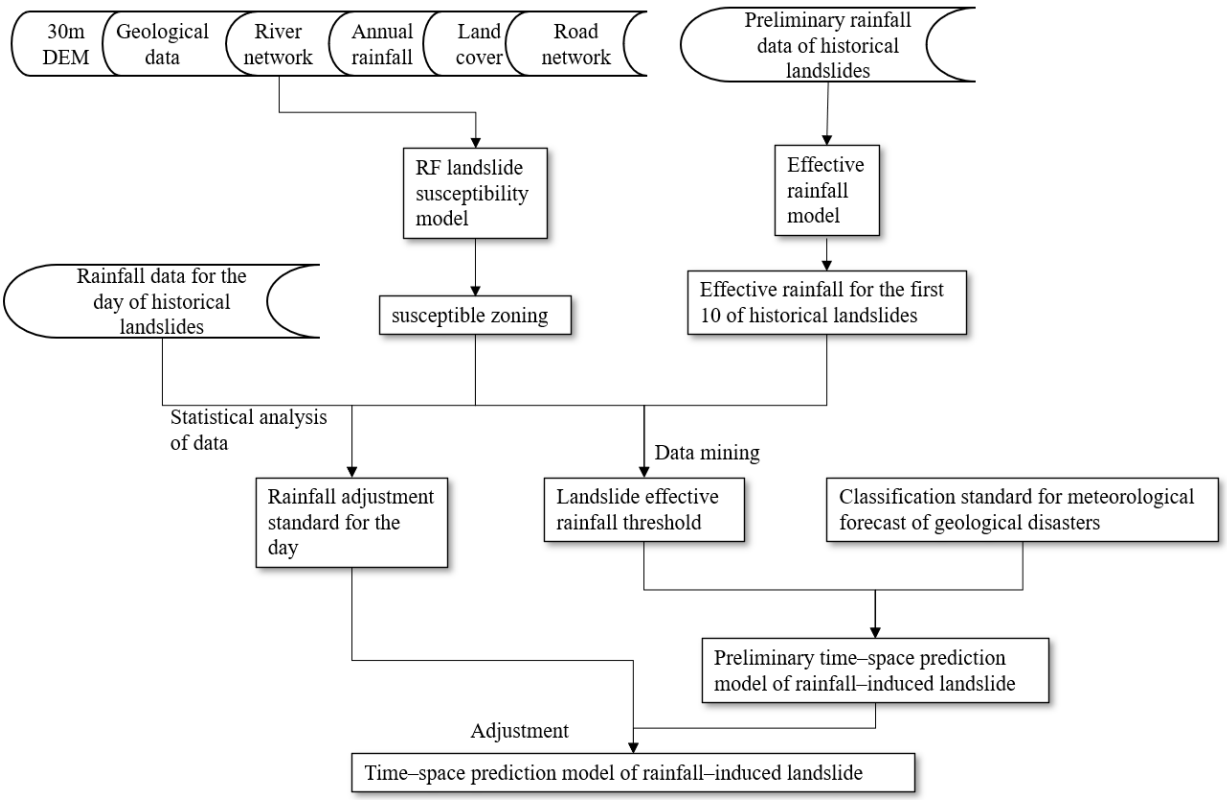


Figure 1. Overall technical route.

2.2. Study Area

Fengjie County is in the north of Chongqing (Figure 2). Fengjie County is located at the junction of the Daba Mountains Arc fold fault zone, the Eastern Sichuan Arc concave fold zone, and the Sichuan, Hunan, and Guizhou Uplift fold zones. Figure 3 shows the

distribution of faults. The tectonic stress field is mainly characterized by near north–south compression, and the tectonic form is mainly folded. The direction of the tectonic line is northeast–east, and the anticline and syncline are parallel. In the whole study area, the main development consists of the Damuya anticline, Qumahe syncline, Soling syncline, Catch-up syncline, Qiyaoshan anticline, Wushan syncline, Hengshi anticline, and the Guandu syncline (Figure 3). It has mountainous landforms. The northeast and southeast regions of Fengjie are higher, and the central and western parts are relatively low-altitude. Its strata are mainly Quaternary (Q), Jurassic (J), Triassic (T), Permian (P), Carboniferous (C), Devonian (D), and Silurian (S). The geological conditions of Fengjie County are complex; most of the areas are mountainous areas, and geological disasters are frequent, large in scale, diverse in variety, and wide in scope, causing great loss of life and property. According to the Köppen–Geiger climate classification [36], the study area has a subtropical humid climate with abundant rainfall and long sunshine duration. The average annual temperature is 18.1 °C, the average annual relative humidity is 71.2%, the average annual precipitation is 1132 mm, and the annual sunshine hours are 1639 h.

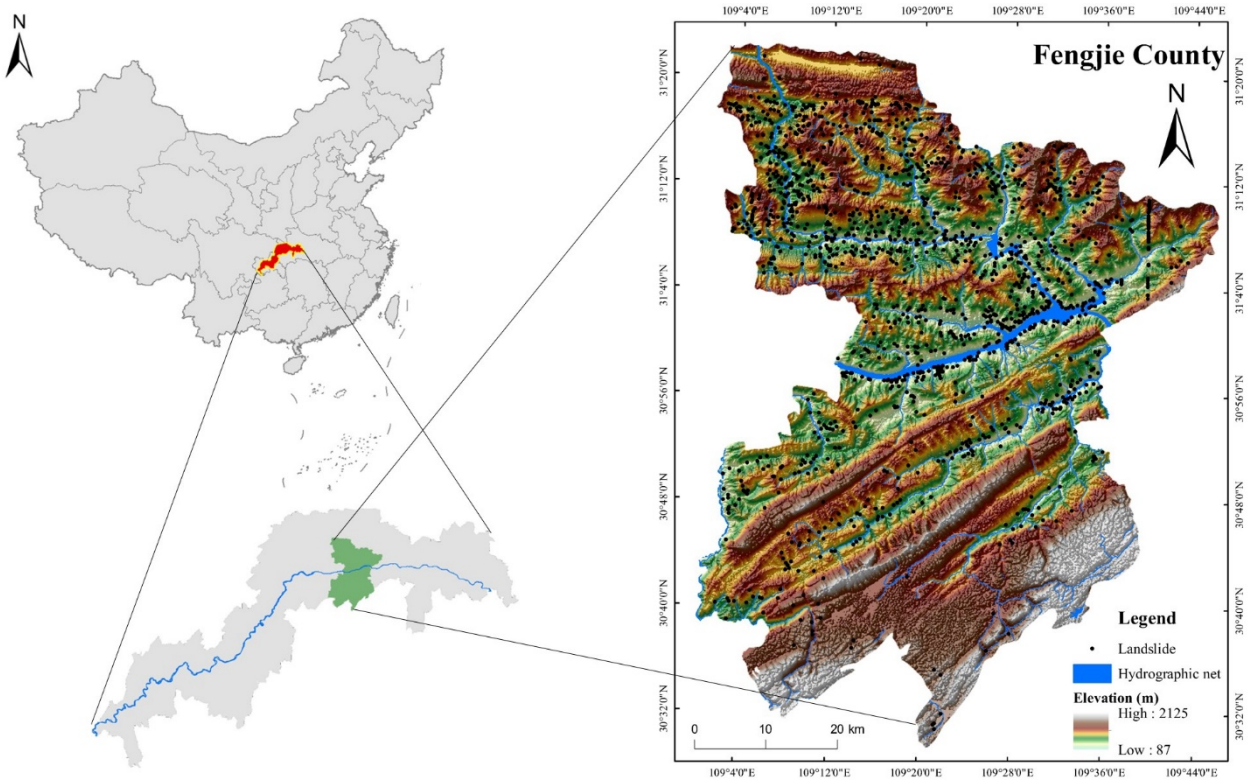


Figure 2. The location of the study area.

Fengjie County has a subtropical monsoon climate with an average annual rainfall of 1132 mm. Most of the landslides in Fengjie County occur from May to October, and the flood season, especially periods of concentrated rainfall, is a time of high incidences of landslide disasters in Fengjie County. Fengjie belongs to the Three Gorges Reservoir Area. The occurrence of landslides is closely related to the reservoir area. The periodic rise and fall of the water level in the reservoir area will cause landslide activity near the reservoir area to show unstable periodicity. The periodical change in reservoir water level will lead to instability of the slope around the reservoir area. In the normal or dry season, the slope is stable or primarily stable. In the flood season or rainstorm period, the slope is saturated, the stability is poor, and the area is prone to landslides [37]. The types and main triggering factors of 1520 historical landslides in Fengjie County from 2001 to 2016 were statistically analyzed (Figure 4). In terms of type, small/shallow/soil landslides account for 82% of the total number of landslides, and large/deep/clay landslides account for only

18%. From the perspective of main triggering factors, rainfall-induced landslides accounted for the majority (75.88%), whereas groundwater (pore water) and human activity-induced landslides accounted for 10.05% and 2.01%, respectively.

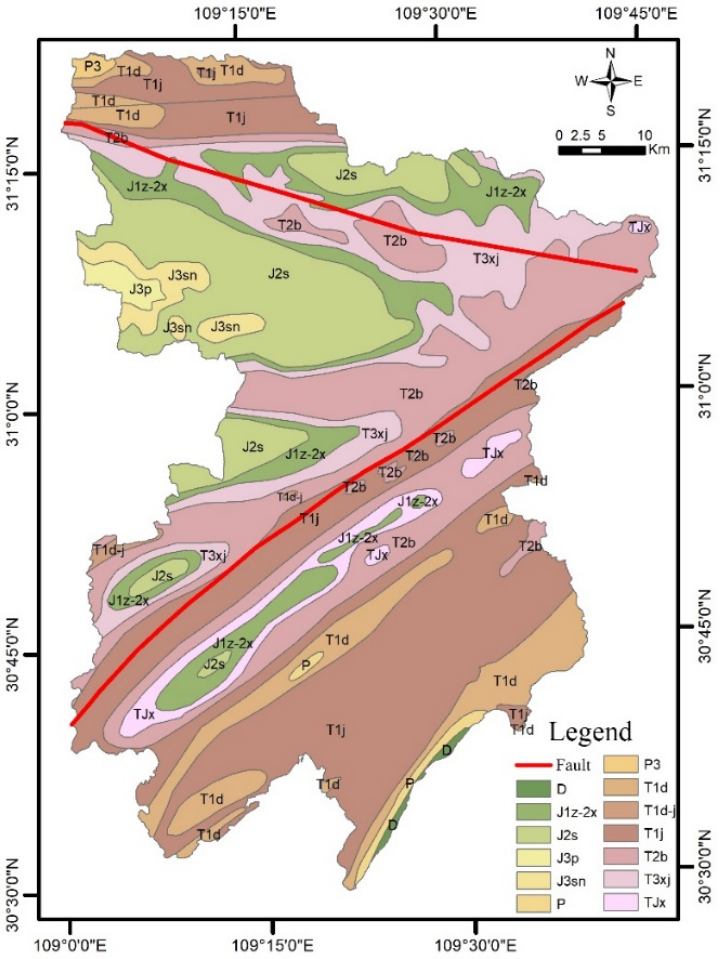


Figure 3. Geological map of the study area.

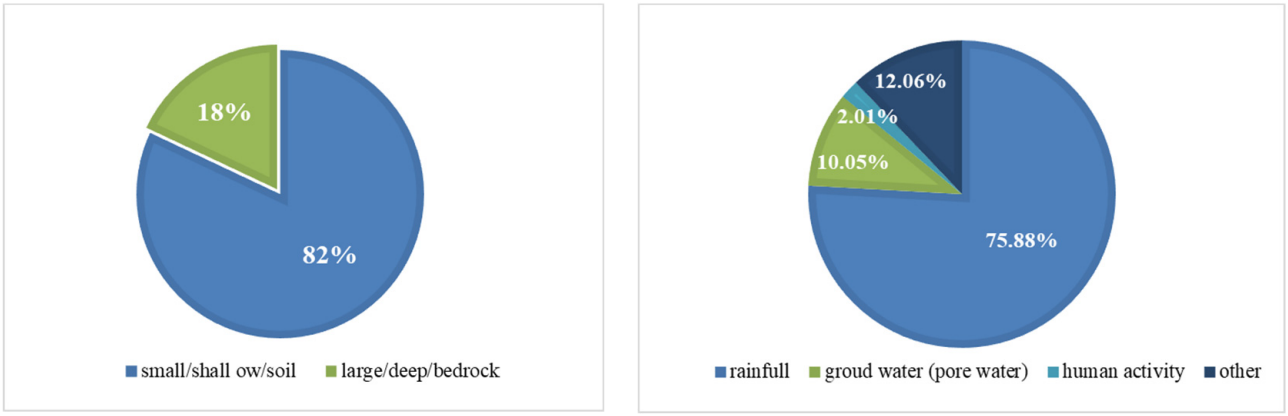


Figure 4. Scale of landslide and trigger: (**a**) landslide type, (**b**) trigger.

As shown in Figure 5, where the average annual rainfall is high (annual average rainfall over 1060 mm), the historical landslides are also densely distributed. According to statistics on historical rainfall-type landslides in Fengjie, the proportion of landslides

occurring in the rainy season (May to October) is more than 90%. This is in good agreement with the concentrated rainfall in Fengjie, and shows that the landslides in this area are positively correlated to precipitation.

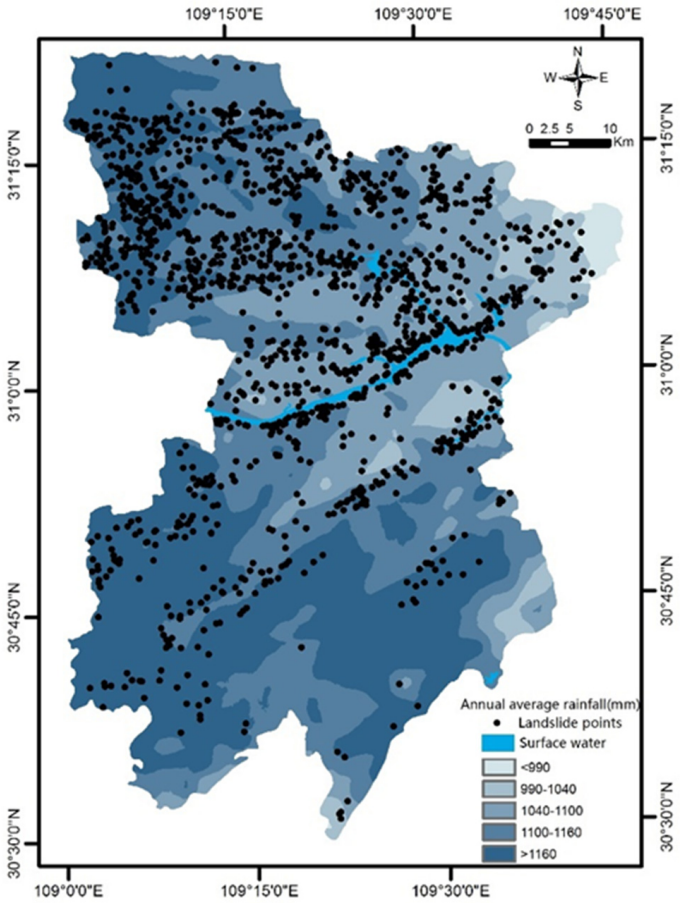


Figure 5. Average rainfall over the years and historical landslides.

The rainfall is extremely uneven and tends to be concentrated in one or several peaks of rainfall intensity, while the rainfall intensity in most other periods is very low or zero. Rainfall pattern analysis was performed on the first four days (96 h) of the occurrence of some rainfall-type landslides in the study area. The 96 h was divided into eight time periods, each of 12 h, and the rainfall in each period was accumulated. Figure 6 shows four typical rainfall patterns in the statistical rainfall-induced landslide data. The following criteria were used to distinguish rainfall patterns. When the peak rainfall occurs in the period 1–2, it is determined to be of the decreasing type; when the peak rainfall occurs in the period 3–6, it is considered to be of the mid-peak type; when it occurs within the 7–8 period, it is considered to be of the increasing type; when there are three or more peak rainfalls, and the difference between them is within 10 mm, it is considered to be of the average type.

According to this standard, of the 284 cases of rainfall-induced landslides, there were 186 cases of increasing rainfall, accounting for 65.5% of the total; 64 cases of mid-peak rainfall, accounting for 22.5% of the total; 19 cases of decreasing rainfall, accounting for 6.7% of the total; and 15 cases of average rainfall, accounting for 5.3% of the total (Figure 7). It can be seen that there was a strong correlation between rainfall and landslides. The impact of rainfall on landslides is not only seen on the day the landslides occur, but also has a certain lag effect on the occurrence of landslides. Therefore, both the rainfall of the day and the previous rainfall have a strong impact on the occurrence of landslides; hence,

the threshold for the occurrence of landslides caused by rainfall is divided according to these two aspects.

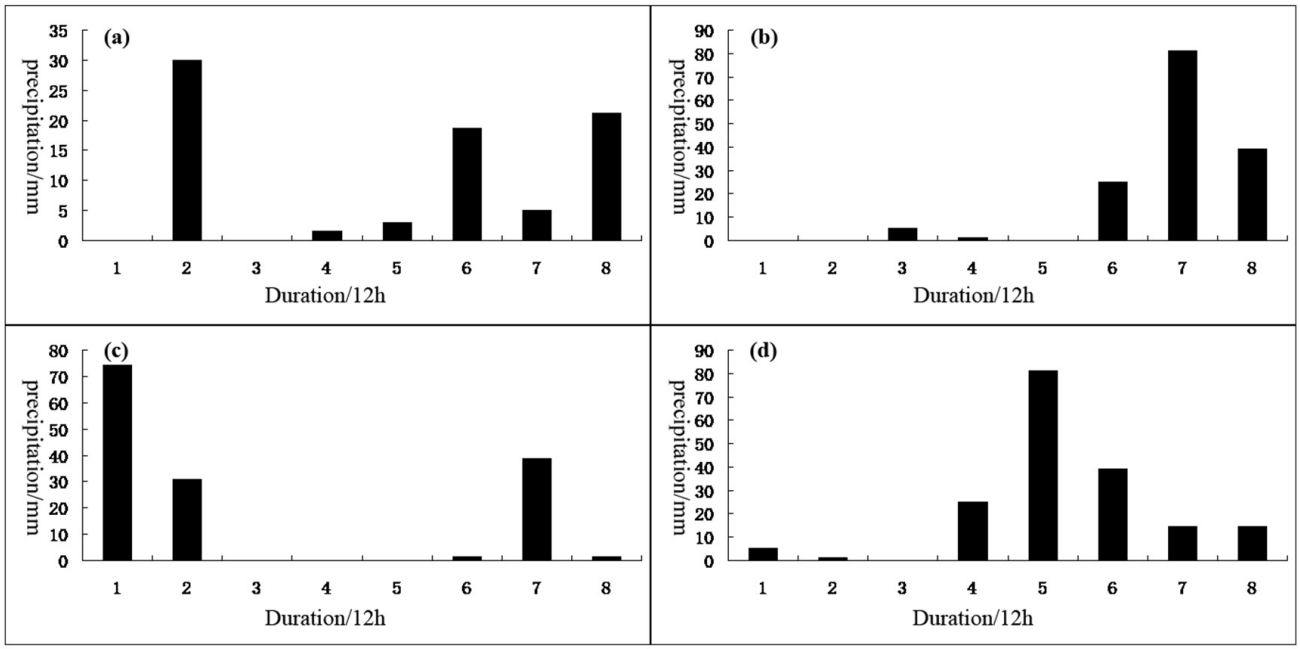


Figure 6. Four typical rainfall patterns in Chongqing: (**a**) average type; (**b**) increasing type; (**c**) diminishing type; (**d**) mid-peak type.

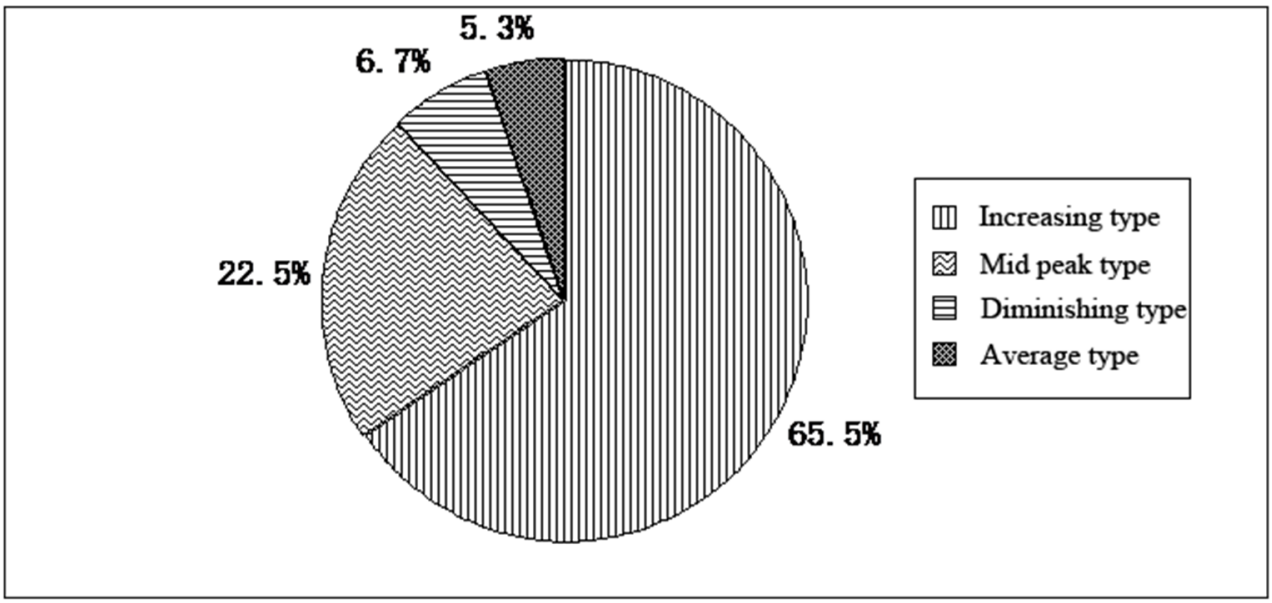


Figure 7. Percentage of four different rainfall types that induce landslides.

2.3. Susceptibility Zoning

2.3.1. Selection of Influencing Factors

Landslides are affected by both natural and human conditions. Based on existing research [38,39] and Fengjie County's landslide development characteristics, this paper selects 16 evaluation factors under the influence of four aspects: topography (elevation, slope, aspect, slope position, profile curvature, landforms, topographic wetness index (TWI)), geology (lithology, distance from fault, combination reclassification of stratum dip direction and slope aspect (CRDS)), environmental conditions (normalized vegetation index

(NDVI), distance from rivers, annual average rainfall, land cover), and human activities (the distance from roads and from buildings). The specific meanings as shown in Table 1.

Table 1. Meanings of influencing factors.

Influencing Factor	Meaning
Elevation	The distance from a point along the vertical line to the base surface
Slope	The degree of steepness of the surface unit
Aspect	The direction of the projection of the slope normal on the horizontal plane
Slope position	The landform part of the slope
Landforms	Relatively small-scale landforms, such as hills, valleys, terraces, etc.
Profile curvature	The rate of change of the surface slope at any point on the ground
TWI	The influence of regional topography on runoff flow direction and accumulation
Lithology	Some attributes that reflect the characteristics of the rock
Distance from faults	The distance to the nearest fault
CRDS	The relationship between rock inclination and slope aspect
NDVI	Percentage of vegetation area to the total statistical area
Distance from rivers	Distance to the nearest river
Land cover	Ways the land is used
Distance from roads	Distance to the nearest road
Distance from buildings	Distance to the nearest house
Annual average rainfall	Average annual rainfall over multiple years

2.3.2. Treatment of Influencing Factors

To reduce the influence of different dimensions, the reclassified data are normalized so that the value is between 0 and 1:

$$X = \frac{X' - X_{min}}{X_{max} - X_{min}} \quad (1)$$

where X is the normalized result, X′ is the original data of each factor, X_{min} is the minimum value of each factor, and X_{max} is the maximum value of each factor.

The influencing factors are reclassified, as shown in Table 2.

Table 2. Influencing factor categories of landslides.

Influencing Factor	Grade	Classification Standard
Elevation/(m)	7	1. <340; 2. 340~595; 3. 595~850; 4. 850~1105; 5. 1105~1360; 6. 1360~1615; 7. >1615
Slope/(°)	6	1. <10°; 2. 10~20°; 3. 20~30°; 4. 30~40°; 5. 40~50°; 6. >50°
Aspect/(°)	9	1. Flat; 2. North; 3. Northeast; 4. East; 5. Southeast; 6. South; 7. Southwest; 8. West; 9. Northwest
Slope position	6	1. Valleys; 2. Lower slope; 3. Flat slope; 4. Middle slope; 5. Upper slope; 6. Ridge
Landforms	10	1. Canyons, Deeply incised streams; 2. Mid-slope drainages, shallow valleys; 3. Upland drainages, headwaters; 4. U-shape valleys; 5. Plains; 6. Open slopes; 7. Upper slopes, mesas; 8. Local ridges, hills in valleys; 9. Mid-slope ridges, small hills in plains; 10. Mountain tops, high narrow ridges
Profile curvature	7	1. −1.0; 2. −1~0.5; 3. −0.5~0; 4. 0~0.5; 5. 0.5~1.0; 6. 1.0~1.5; 7. >1.5
TWI	7	1. <10; 2. 10~12; 3. 12~14; 4. 14~16; 5. 16~18; 6. 18~20; 7. >20
Lithology	7	1. TJx; 2. T1j; 3. D; 4. T1d-j; 5. J2s, J1z-2x, J3sn, J3p; 6. T1d, T3xj, T2b; 7. P, P3

Table 2. *Cont.*

Influencing Factor	Grade	Classification Standard
Distance from faults/(m):	11	1. <100; 2. 100~200; 3. 200~300; 4. 300~400; 5. 400~500; 6. 500~600; 7. 600~700; 8. 700~800; 9. 800~900; 10. 900~1000; 11. >1000
CRDS	6	1. Bedding slope; 2. Skewed slope; 3. Inclined slope; 4. Horizontal; 5. Reverse slope; 6. Flat
NDVI	7	1. <0.10; 2. 0.10~0.20; 3. 0.20~0.30; 4. 0.30~0.40; 5. 0.40~0.50; 6. 0.50~0.60; 7. >0.60
Distance from rivers/(m)	7	1. <100; 2. 100~200; 3. 200~300; 4. 300~400; 5. 400~500; 6. 500~600; 7. >600
Land cover	6	1. Cultivated land; 2. Woodland; 3. Meadow; 4. Land used for building; 5. Water area; 6. Unused land
Distance from roads/(m)	7	1. <100; 2. 100~200; 3. 200~300; 4. 300~400; 5. 400~500; 6. 500~600; 7. >600
Distance from buildings/(m)	7	1. <100; 2. 100~200; 3. 200~300; 4. 300~400; 5. 400~500; 6. 500~600; 7. >600
Annual average rainfall/(mm)	5	1. <990; 2. 990~1040; 3. 1040~1100; 4. 1100~1160; 5. >1160

2.3.3. Random Forest

Random forest is a classifier that uses multiple decision trees to train and predict samples. When using data subsets to construct a decision tree, elements of different data subsets can be repeated (that is, sampling with replacement). The random forest can reduce the one-sidedness and inaccuracy problems of single decision tree prediction, and prevent the judgment result of a single decision tree from overfitting, resulting in lower prediction accuracy. The remaining samples can be used as a test set to judge the error rate of the model prediction:

$$Y(x) = \arg \max_{z} \sum_{i=1}^{k} I(y_i(x) = Z) \quad (2)$$

where Y(x) represents the judgment result of the RF model, $y_i(x)$ represents a single-course DT (decision tree), and Z represents the variable.

2.3.4. Accuracy Verification

The accuracy of the model prediction results can be determined by the receiver operating curve (ROC). The curve is obtained by setting a probability threshold to obtain a series of different binary classification results, and is then compared with the actual results. The closer the ROC is to the upper left, the higher the accuracy of the model. The point of the ROC closest to the upper left corner is the best threshold with the fewest errors, as well as the lowest total number of false positives and false negatives. The area under the curve (AUC) value is the area covered by the ROC, which can quantitatively determine the accuracy of the model. The AUC value is between 0 and 1, and the larger the value, the higher the model accuracy.

The accuracy of the model is verified; with the AUC value of the model training set to 0.95 and the AUC value of the test set to 0.87, the overall accuracy is 0.93 (Figure 8). The three values are all greater than 0.85, indicating the accuracy of the model. Higher accuracy means a better predictive ability, such that it can be used for landslide research.

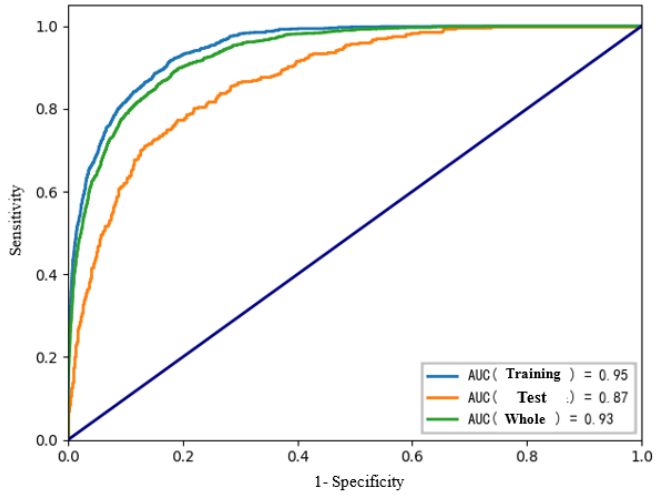


Figure 8. Model ROC curve.

2.4. Fractal Model of Antecedent Effective Precipitation

The triggering of landslides is not only related to the precipitation on the day, but also to the effective precipitation of the previous period. Existing studies [40,41] have shown that the cumulative precipitation of the previous period is positively correlated with the frequency of landslides. The greater the accumulated precipitation, the greater the probability of landslides. Due to the effects of interception, evaporation, and seepage, the previous rainfall does not directly act on the slope. In this paper, the precipitation after the attenuation of the previous cumulative rainfall is used as an important parameter for landslide warning and prediction. The effective precipitation of the previous period is the weighted sum of the daily precipitation of the previous period. The weight here is the attenuation coefficient β. The formula for the calculation of the fractal relationship is:

$$\beta = \sum_{n=1}^{m} \left(1 - \left(\frac{n}{n+1}\right)^{\alpha}\right) \tag{3}$$

where n represents the number of days before the occurrence of the landslide; m represents the number of days; and α is the scale index, determined by the formula Rn = C(n + 1)a, where C is the coefficient and the formula is the cumulative precipitation threshold fractal curve, which can be studied by analyzing the regional landslide. The relationship between the occurrence and the cumulative precipitation threshold is derived.

2.5. Hybrid Model of the Antecedent Effective Precipitation and the Daily Precipitation under the Susceptibility Zoning

2.5.1. Threshold Model Based on Susceptibility Zoning and Antecedent Effective Precipitation

According to the China Geological Hazard Meteorological Forecast and Early Warning Implementation Plan [42], the geological hazard weather forecast is divided into four levels: blue, yellow, orange, and red. We sorted the effective precipitation in the five different susceptibility regions in the study area, from very low to very high, and formed a first-order matrix. When the cumulative frequency of landslides in each landslide-prone area reached 25%, 40%, and 55%, the corresponding effective precipitation was used as the effective precipitation threshold for the yellow, orange, and red warnings.

$$Yi = \begin{cases} 0, \ (J < Y_{yellow}) \\ 1, \ (Y_{yellow} \le J < Y_{orange}) \\ 2, \ (Y_{orange} \le J < Y_{red}) \\ 3, \ (Y_{red} \le J) \end{cases} \tag{4}$$

where Y_{yellow} is a yellow warning value with a cumulative frequency of 25%, Y_{orange} is an orange warning value with a cumulative frequency of 40%, Y_{red} is a red warning value with a cumulative frequency of 55%, and Y_i is the actual antecedent effective precipitation.

$$Ym = X_{fm} \quad (5)$$

where Y_m is the early warning threshold; X_{fm} is the effective precipitation when the cumulative frequency of the landslide reaches a certain amount, which is expressed in matrix form, and the internal size is arranged from small to large; m is yellow, orange, or red; and fm is the cumulative frequency of landslides corresponding to the serial number.

$$fm = [l_i * n] \quad (6)$$

where fm is the serial number corresponding to the cumulative frequency of the landslides; $i =$ yellow, orange, or red; $l_{yellow} = 25\%$, $l_{orange} = 40\%$, and $l_{red} = 55\%$; n is the total number of landslides in each group; and [] refers to an integer.

2.5.2. Analysis of Early Warning and Forecast of Landslide Coupled with Daily Precipitation

The effect of the antecedent effective precipitation on the occurrence of landslides is a cumulative process, while daily precipitation has a triggering effect. Therefore, according to the zoning of landslide susceptibility, mathematical statistics and data mining are performed based on the cumulative amount of 24 h precipitation and the frequency of landslides, and the results are adjusted. The specific process is shown in Figure 9.

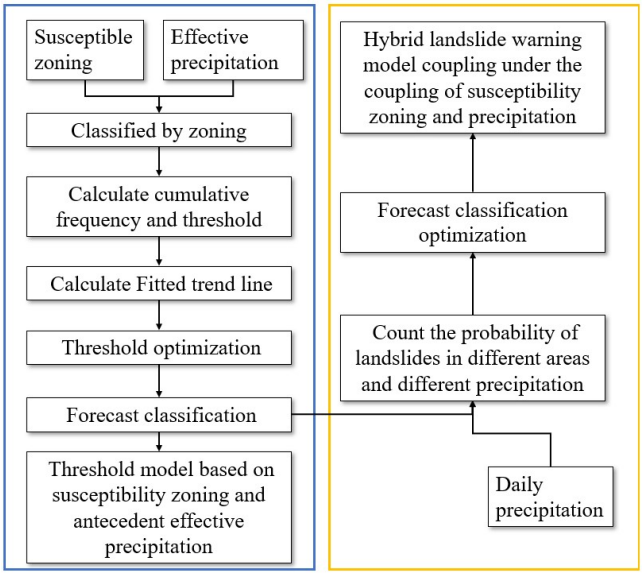


Figure 9. Specific flow chart4. Results and Discussion.

Based on the susceptibility zone and rainfall data, the rainfall data of the 10 days before the landslide in each zone were sorted, the attenuation coefficient of the previous rainfall was calculated, and the rainfall was corrected by this coefficient. We chose yellow, orange, and red as the three warning levels. The rainfall values corresponding to the first 25%, 40%, and 55% of landslide occurrence frequencies in each susceptibility zone were calculated as the thresholds for different grades of previous effective rainfall. When coupling the daily rainfall, we added a blue color to the warning level. The coupling followed certain rules: if the daily rainfall is less than a certain level, no adjustment will be made; when the daily rainfall is greater than a certain level, the warning level needs to be increased; the improvement may be of one level or multiple levels; the daily rainfall thresholds, adjusted by the warning levels of different susceptibility zones, are different.

3. Result

3.1. Random Forest Susceptibility Evaluation

The accuracy of the model prediction results can be determined by the ROC. The closer the curve is to the upper left, the higher the accuracy of the model. The AUC value is the area covered by the ROC curve, which can be quantified to judge the accuracy of the model; the AUC value is between 0 and 1, and the larger the value, the higher the accuracy of the model.

The accuracy of the model is verified; with the AUC value of the model training set to 0.95 and the AUC value of the test set to 0.87, the overall accuracy is 0.93 (Figure 8). These three values are all greater than 0.85, indicating the high accuracy of the model. A model with this level of predictive ability can be used for landslide research.

The random forest model was used to evaluate the landslide susceptibility of the study area, and the range was graded by the results of the natural breakpoint method. After grading, the Landslide Susceptibility Mapping (LSM) result was obtained. As shown in Figure 10, the majority of study areas are in regions with low or very low landslide susceptibility, and are concentrated in the south and southeast; highly prone areas are concentrated on both banks of the Yangtze River and its tributaries, mainly in the north and central regions of Fengjie.

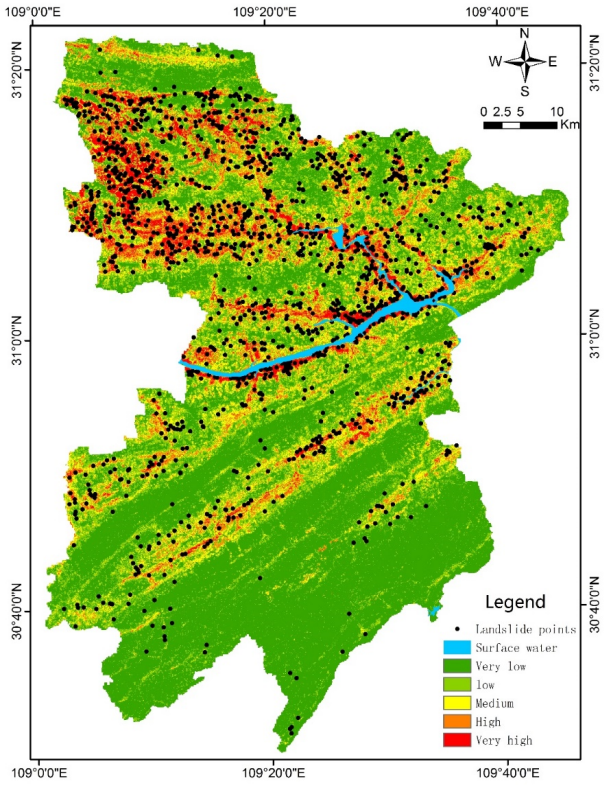


Figure 10. Landslide susceptibility zoning map.

3.2. Antecedent Effective Precipitation Model

Based on 1520 landslides with clear occurrence dates and coordinate records induced by precipitation in the Fengjie area from 2003 to 2016, and the daily precipitation data of the 10 days before the landslide (the day, the day before, the first three, five, and ten days of each landslide, and five other periods of cumulative precipitation), sorted by cumulative precipitation from small to large, we calculated the cumulative precipitation corresponding to 75% and 90% of the cumulative frequency of landslides, and took this as the cumulative precipitation threshold for different landslide occurrence probabilities (Table 3).

Table 3. Influencing factor categories of landslides.

Precipitation/mm / Cumulative Frequency of Landslides/%	The Landslide Day	From the Day of the Landslide to 3 Days before	From the Day of the Landslide to 5 Days before	From the Day of the Landslide to 10 Days before
75	69.9	146.4	252.9	273.4
90	92.7	233.2	330.7	372.3
Difference	22.8	86.8	77.8	98.9

Figure 11 uses the observation period (days) as the abscissa and the cumulative precipitation threshold as the ordinate to display the cumulative precipitation threshold for each observation period. The accumulated precipitation is the power exponential function of the observation period (n), and values of α can be calculated by fitting, which were found to be 0.609 (75% landslide probability) and 0.603 (90% landslide probability).

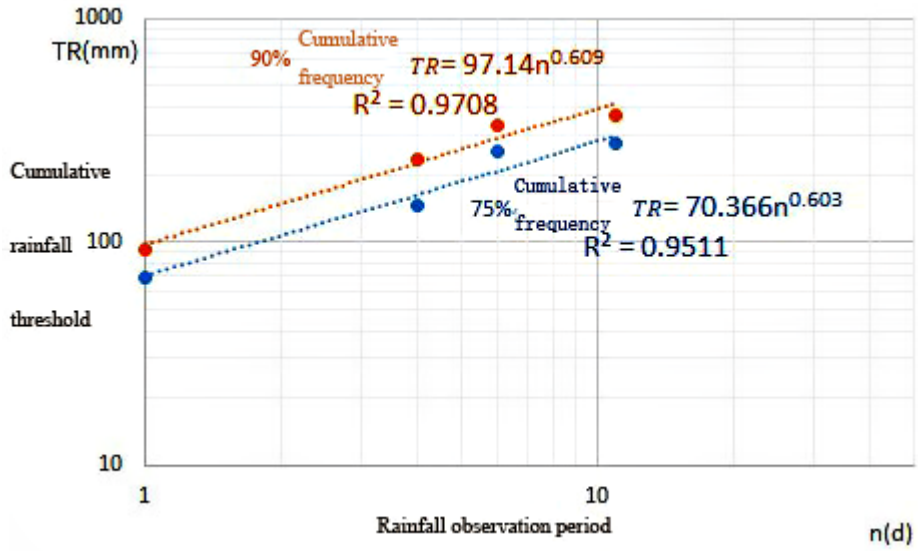


Figure 11. The relationship between the cumulative precipitation threshold and the number of days of the observation period.

Substituting α into Equation (3), we calculated the attenuation coefficient of the daily precipitation in the 10 days prior to the landslide. Table 4 presents the attenuation coefficients of the previous precipitation events, corresponding to 90% of the cumulative frequency of the landslide.

Table 4. Antecedent rain attenuation coefficient.

	1 Day before	2 Days before	3 Days before	4 Days before	5 Days before	6 Days before	7 Days before	8 Days before	9 Days before	10 Days before
90%	0.344	0.219	0.161	0.127	0.105	0.090	0.078	0.069	0.062	0.056

3.3. Calculation and Adjustment of Antecedent Effective Precipitation Threshold Based on Susceptibility Zoning

3.3.1. Threshold Model Based on Susceptibility Zoning and Antecedent Effective Precipitation

According to the antecedent effective precipitation model and susceptibility zoning, the precipitation thresholds of historical landslides were counted. The results are shown in Table 5. The expressions of the three fitting lines of yellow, orange, and red warning levels are: Y = –6.1687x + 134.03, Y = –14.283x + 132.09, and Y = –18.954x + 108.83 (x = 1, 2, 3, 4,

or 5, corresponding to very low areas, low areas, moderate areas, high areas, or very high areas, respectively).

Table 5. Effective precipitation thresholds in the first 10 days of different susceptibility zones and different warning levels.

Susceptibility Zoning	Frequency of Landslides	Effective Precipitation in the First 10 Days (mm)	Warning Level
Very low	25%	96	Yellow
	40%	129	Orange
	55%	137	Red
Low	25%	58	Yellow
	40%	87	Orange
	55%	114	Red
Moderate	25%	51	Yellow
	40%	87	Orange
	55%	109	Red
High	25%	49	Yellow
	40%	87	Orange
	55%	109	Red
Very high	25%	6	Yellow
	40%	58	Orange
	55%	109	Red

The original precipitation threshold was adjusted according to the trend line; the optimized precipitation thresholds of each level after calculation are shown in Table 6.

Table 6. Thresholds after adjustment of the effective precipitation in the early stage of different susceptibility zones and different warning levels.

Warning Level	Very Low Areas (mm)	Low Areas (mm)	Moderate Areas (mm)	High Areas (mm)	Very High Areas (mm)
Yellow	90	71	52	33	14
Orange	118	104	89	75	61
Red	128	122	116	109	103

3.3.2. Warning Model Coupled with Daily Precipitation

We performed statistical analysis on the daily precipitation data of 1520 landslides, and obtained the specific adjustment methods of the coupled day's precipitation threshold model, as follows: (1) We counted the cumulative frequency of landslide occurrence, from small to large, unaffected to landslide-prone areas. (2) The cumulative frequency of landslides was less than 0.4. The corresponding daily precipitation type and warning level was not adjusted. For the daily precipitation type corresponding to a cumulative frequency greater than 0.4 and less than 0.7, the warning level was raised by one level; for the daily precipitation type corresponding to a cumulative frequency greater than 0.7, the warning level was raised by 2. (3) We increased the level until the red warning level. Table 7 shows the relationship between the original forecast level and the adjusted level.

Table 7. Forecast level adjustment based on the precipitation of the day.

Original Warning Level	Very Low Areas	Low Areas	Moderate Areas	High Areas	Very High Areas
Blue	Blue	Blue	Blue	Yellow (Light rain)	Orange (Light rain)
Yellow	Yellow	Yellow	Yellow	Orange (Heavy rain)	Orange (Light rain)
Orange	Red (rainstorm)	Red (Heavy rain)	Red (Heavy rain)	Red (Heavy rain)	Red (Heavy rain)
Red	Red	Red	Red	Red	Red

3.4. Instance Verification

3.4.1. Regional Verification Analysis

Figure 12a is a landslide warning map generated based on the antecedent effective precipitation data and landslide susceptibility zoning data of various weather stations on 30 June 2018. Figure 12b is a landslide warning map based on the antecedent effective precipitation data of each weather station on 30 June 2018, and the daily precipitation data, combined with the landslide susceptibility zoning.

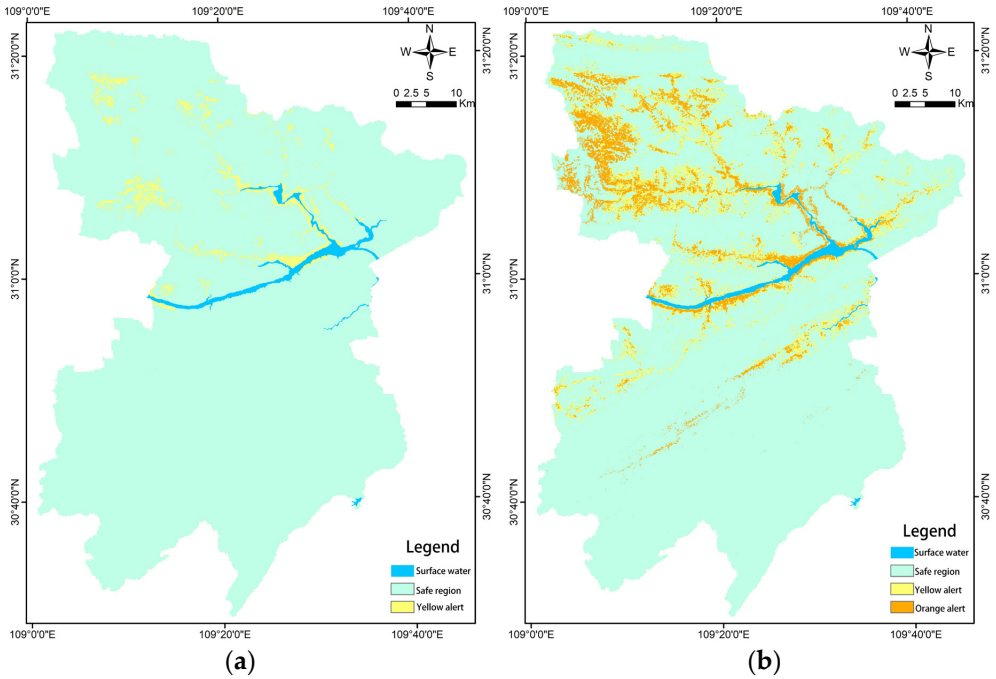


Figure 12. Early warning map of landslide area: (**a**) early warning results based on susceptibility zoning and antecedent effective precipitation; (**b**) early warning results based on a coupled day precipitation.

Most of the study areas were in the warning range, while Fengjie County was mainly in the safe area. Compared with the single early precipitation landslide warning, the coupled precipitation landslide warning model has an orange warning. What is more, in the single landslide warning model, most of the yellow warning areas are replaced by orange warnings, and the yellow warnings in the coupled warning model are attached to the orange warnings.

3.4.2. Monomer Verification Analysis

The rainfall-induced catastrophic deformation of the above five typical landslides can be summarized, as shown in Table 8 below, and their spatial locations are shown in Figure 13. The final analysis results of the five typical cases are yellow to red warnings. All five landslides on the site experienced large deformations due to rainfall, but there was no

overall instability damage. Therefore, the overall early warning result is consistent with the actual situation on the ground.

Table 8. Summary table of early warning analysis of typical cases of precipitation-induced landslides in 2017.

Number	Name	Susceptibility Zoning	Antecedent Precipitation (mm)	Daily Precipitation (mm)	Warning Level			Actual Catastrophe
					Antecedent Precipitation	Daily Precipitation	Adjusted Level	
1	Damian	Very high	47.6	85.86	Safe	Yellow	Yellow	Continuous deformation
2	Hejiawan	Very high	12.32	147.5	Safe	Red	Red	Continuous deformation Small area collapse New deformation crack
3	Huoshitan	Very high	88.38	0	Orange	Blue	Orange	Continuous deformation Multiple cracks
4	Zhakou	High	93.8	1.4	Orange	Blue	Orange	Continuous deformation Multiple cracks
5	Xinpu	High	52.26	0	Yellow	Blue	Yellow	Local deformation

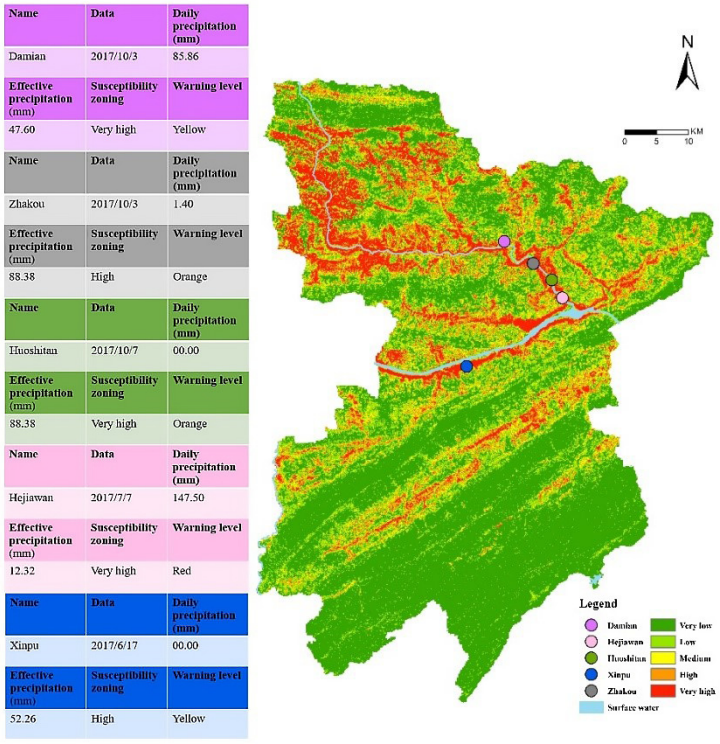


Figure 13. Distribution map of 5 landslide cases in 2017.

The established landslide warning model with the coupling of susceptibility zoning and precipitation was applied to the newly occurring precipitation-induced landslides in the study area and obtained a good verification effect, which is primarily in line with the actual situation.

4. Discussion

4.1. The Importance and Influence of Factors

The contributions of factors to landslides are different. The detection of landslide-inducing factors can provide an important reference for landslide disaster prediction. In this paper, the importance of 16 factors in the model is detected using the reduced Gini index in the random forest model (Figure 14). The highest contributors to landslides are annual average rainfall and elevation.

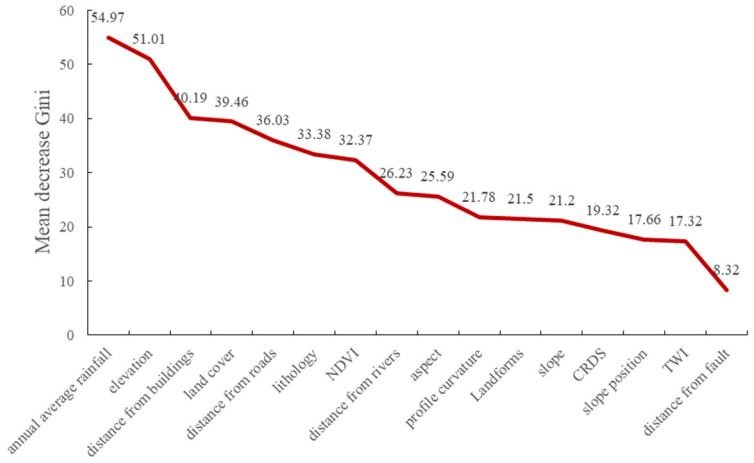
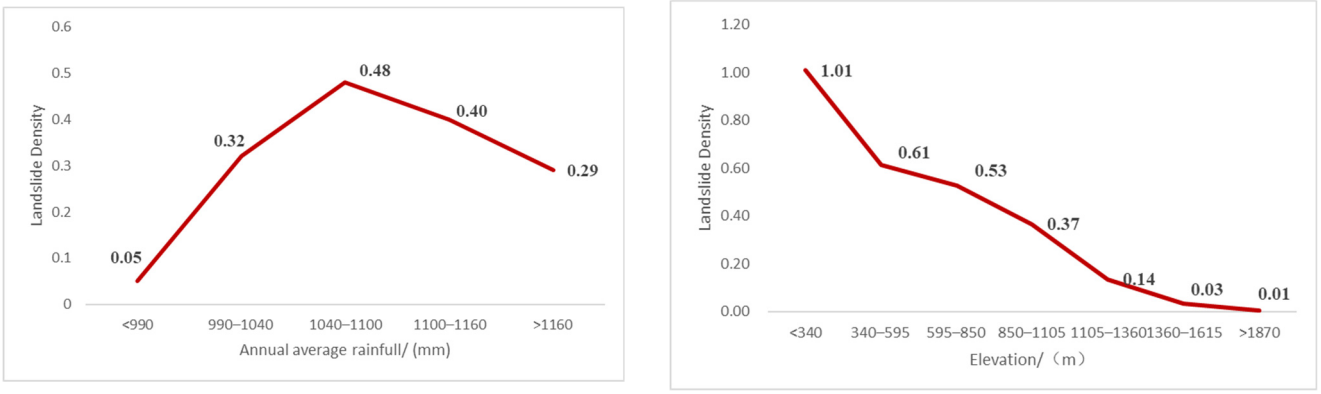


Figure 14. Importance of landslide influencing factors.

The statistical distributions of landslide density based on these two factors are presented in Figure 15. Annual average rainfall is the most important factor. According to the statistics of annual average rainfall and landslide density, the landslide density first increases and then decreases with the increase in annual average rainfall. Because the surface runoff formed by rainfall takes away the unstable soil particles on the slope, the slope is eroded. Rainfall also promotes the growth of local vegetation, thereby inhibiting soil erosion and landslides. Landslide density is negatively correlated with elevation because, usually, in low altitude areas, population agglomeration and human activities easily change the local geological environment, destroy the stability of the slope toe, and lead to a high probability of landslide occurrence.



(**a**) (**b**)

Figure 15. Partial effects on landslide susceptibility of typical conditioning factors: (**a**) annual average rainfall, (**b**) elevation.

4.2. Effectiveness of Antecedent Rainfall

Early rainfall can reduce the adsorption capacity, and increase the pore pressure, of soil, thereby reducing the stability of slope, which is an important factor in terms of inducing landslides. The force of early rainfall on the slope is greatly affected by seasonality. Rainfall and evapotranspiration are also different in different seasons. In the rainy season, large amounts of rainfall and low evaporation rates lead to poor slope stability. However, the increase in evapotranspiration from late spring to early autumn resulted in the decrease in soil pressure and the increase in slope stability. Therefore, this paper accounted for the rainfall 10 days before the landslide, referred to as the effective rainfall in the early stage, so as to avoid invalid rainfall, such as evapotranspiration, being included in the model.

4.3. Practical Application of Coupling Model of Susceptibility Zoning and Precipitation

The influence of rainfall on landslide has hysteresis and effectiveness, which cannot only be studied from the antecedent effective precipitation threshold or the daily precipitation threshold. Therefore, the author proposes a model coupling the antecedent effective precipitation and the daily precipitation, in which the antecedent effective precipitation and the daily precipitation complement each other. Based on the landslide susceptibility zoning, we use the coupling method of the antecedent effective precipitation and the daily precipitation to improve the warning ability of the rainfall threshold model. It was found that the warning level of the coupling model is higher than that of the single model, and the warning range is more realistic. Firstly, according to the landslide susceptibility zoning, the antecedent effective precipitation thresholds of three warning levels (yellow, orange, and red) are given. The antecedent effective precipitation alone is not enough to reflect the real-time impact of rainfall on landslides. Therefore, the actual effect of rainfall on landslides is reflected by coupling the daily precipitation with the antecedent effective precipitation threshold.

According to the example verification (Table 8), the susceptibility area of Hejiawan is divided into middle–high susceptibility areas. After the superposition of antecedent effective precipitation of 47.6 mm, the antecedent effective precipitation warning level is 'safe', but combined with the daily precipitation of 85.89 mm, the warning level of Hejiawan landslide is 'red', which is consistent with the actual situation of small-area landslides. The daily precipitation of Huoshitan and Xinpu landslides is 0, and the possibility of landslide occurrence is low. However, combined with the antecedent effective precipitation, the forecast grades of these two places are 'orange' and 'yellow'. The results show that the coupling model of the antecedent effective and the daily precipitation can avoid the occurrence, and reduce the risk, of landslides.

5. Conclusions

In this study, we propose a new precipitation warning model that couples landslide susceptibility, antecedent effective precipitation, and the daily precipitation threshold. We applied the model to actual landslide cases and verified it to explain the practicality and accuracy of the model. Our conclusions are as follows:

(1) The evaluation results of the landslide susceptibility model in Fengjie County based on RF are accurate and reasonable. The AUC value of the test set is 0.87, and the annual average rainfall and elevation are the factors that contribute the most to the model.
(2) The early warning model of landslide susceptibility, the antecedent effective precipitation, and the daily precipitation coupling has higher accuracy than the model of landslide susceptibility and the antecedent effective precipitation coupling, and it can better characterize the mechanism of rainfall-induced landslides.
(3) The landslide warning model based on random forest coupling of rainfall-inducing factors in landslide susceptibility zoning has high warning accuracy, which can provide a reference for areas with the same geological conditions and climatic conditions.

Author Contributions: Conceptualization, H.W. and D.S.; formal analysis, H.W., D.S., Q.G., S.S., C.M. and F.Z.; data curation, Q.G. and S.S.; investigation, H.W., C.M. and F.Z.; writing—original draft, D.S., and Q.G.; writing—review, and editing H.W. and D.S. All authors have read and agreed to the published version of the manuscript.

Funding: This research was funded by the National Natural Science Foundation of China (Grant No.41901214), National Key Research and Development Program of China (Grant No. 2018YFC1505501), the Natural Science Foundation of Chongqing (Grant No. cstc2020jcyjmsxmX0841), and Scientific and Technological Research Program of Chongqing Municipal Education Commission (Grant No. KJQN201800511).

Conflicts of Interest: The authors declare no conflict of interest.

References

1. Huang, F.; Yin, K.; Huang, J.; Gui, L.; Wang, P. Landslide susceptibility mapping based on self-organizing-map network and extreme learning machine. *Eng. Geol.* **2017**, *223*, 11–22. [CrossRef]
2. Chen, L.; Mei, L.; Zeng, B.; Yin, K.; Shrestha, D.P.; Du, J. Failure probability assessment of landslides triggered by earthquakes and rainfall: A case study in Yadong County, Tibet, China. *Sci. Rep.* **2020**, *10*, 16531. [CrossRef] [PubMed]
3. Corominas, J.; van Westen, C.; Frattini, P.; Cascini, L.; Malet, J.P.; Fotopoulou, S.; Catani, F.; Van Den Eeckhaut, M.; Mavrouli, O.; Agliardi, F.; et al. Recommendations for the quantitative analysis of landslide risk. *Bull. Eng. Geol. Environ.* **2013**, *73*, 209–263. [CrossRef]
4. Carrara, A.; Merenda, L. Landslide inventory in northern Calabria, southern Italy. *Geol. Soc. Am. Bull.* **1976**, *87*, 1153–1162. [CrossRef]
5. Fausto, G.; Alberto, C.; Mauro, C.; Reichenbach, P. Landslide hazard evaluation: A review of current techniques and their application in a multi-scale study, Central Italy. *Geomorphology* **1999**, *31*, 181–216.
6. Robert, S.; Westen, C.J.V. Slope instability Recognition, analysis and zonation. *Landslides Investig. Mitig.* **1996**, *247*, 129–177.
7. Di Napoli, M.; Carotenuto, F.; Cevasco, A.; Confuorto, P.; Di Martire, D.; Firpo, M.; Pepe, G.; Raso, E.; Calcaterra, D. Machine learning ensemble modelling as a tool to improve landslide susceptibility mapping reliability. *Landslides* **2020**, *17*, 1897–1914. [CrossRef]
8. Lombardo, L.; Opitz, T.; Ardizzone, F.; Guzzetti, F.; Huser, R. Space-time landslide predictive modelling. *Earth-Sci. Rev.* **2020**, *209*, 103318. [CrossRef]
9. Komori, D.; Rangsiwanichpong, P.; Inoue, N.; Ono, K.; Watanabe, S.; Kazama, S. Distributed probability of slope failure in Thailand under climate change. *Clim. Risk Manag.* **2018**, *20*, 126–137. [CrossRef]
10. Chen, W.; Peng, J.; Hong, H.; Shahabi, H.; Pradhan, B.; Liu, J.; Zhu, A.X.; Pei, X.; Duan, Z. Landslide susceptibility modelling using GIS-based machine learning techniques for Chongren County, Jiangxi Province, China. *Sci. Total Environ.* **2018**, *626*, 1121–1135. [CrossRef]
11. Dou, J.; Yunus, A.P.; Tien Bui, D.; Merghadi, A.; Sahana, M.; Zhu, Z.; Chen, C.W.; Khosravi, K.; Yang, Y.; Pham, B.T. Assessment of advanced random forest and decision tree algorithms for modeling rainfall-induced landslide susceptibility in the Izu-Oshima Volcanic Island, Japan. *Sci. Total Environ.* **2019**, *662*, 332–346. [CrossRef] [PubMed]
12. Kuradusenge, M.; Kumaran, S.; Zennaro, M. Rainfall-Induced Landslide Prediction Using Machine Learning Models: The Case of Ngororero District, Rwanda. *Int. J. Environ. Res. Public. Health* **2020**, *17*, 4147. [CrossRef] [PubMed]
13. Lai, J.S.; Tsai, F. Improving GIS-based Landslide Susceptibility Assessments with Multi-temporal Remote Sensing and Machine Learning. *Sensors* **2019**, *19*, 3717. [CrossRef]
14. Tien Bui, D.; Tuan, T.A.; Klempe, H.; Pradhan, B.; Revhaug, I. Spatial prediction models for shallow landslide hazards: A comparative assessment of the efficacy of support vector machines, artificial neural networks, kernel logistic regression, and logistic model tree. *Landslides* **2016**, *13*, 361–378. [CrossRef]
15. Sun, D.; Xu, J.; Wen, H.; Wang, Y. An Optimized Random Forest Model and Its Generalization Ability in Landslide Susceptibility Mapping: Application in Two Areas of Three Gorges Reservoir, China. *J. Earth Sci.* **2020**, *31*, 1068–1086. [CrossRef]
16. Moayedi, H.; Mehrabi, M.; Mosallanezhad, M.; Rashid, A.S.A.; Pradhan, B. Modification of landslide susceptibility mapping using optimized PSO-ANN technique. *Eng. Comput-Ger.* **2019**, *35*, 967–984. [CrossRef]
17. Pourghasemi, H.R.; Rahmati, O. Prediction of the landslide susceptibility: Which algorithm, which precision? *Catena* **2018**, *162*, 177–192. [CrossRef]
18. Zhou, X.; Wen, H.; Li, Z.; Zhang, H.; Zhang, W. An interpretable model for the susceptibility of rainfall-induced shallow landslides based on SHAP and XGBoost. *Geocarto Int. TGEI* **2022**, 1–27. [CrossRef]
19. Chen, W.; Xie, X.; Wang, J.; Pradhan, B.; Hong, H.; Bui, D.T.; Duan, Z.; Ma, J. A comparative study of logistic model tree, random forest, and classification and regression tree models for spatial prediction of landslide susceptibility. *Catena* **2017**, *151*, 147–160. [CrossRef]
20. Sun, D.; Xu, J.; Wen, H.; Wang, D. Assessment of landslide susceptibility mapping based on Bayesian hyperparameter optimization: A comparison between logistic regression and random forest. *Eng. Geol.* **2021**, *281*, 105972. [CrossRef]
21. Trigila, A.; Iadanza, C.; Esposito, C.; Scarascia-Mugnozza, G. Comparison of Logistic Regression and Random Forests techniques for shallow landslide susceptibility assessment in Giampilieri (NE Sicily, Italy). *Geomorphology* **2015**, *249*, 119–136. [CrossRef]
22. Tsangaratos, P.; Ilia, I.; Hong, H.; Chen, W.; Xu, C. Applying Information Theory and GIS-based quantitative methods to produce landslide susceptibility maps in Nancheng County, China. *Landslides* **2016**, *14*, 1091–1111. [CrossRef]
23. Alvioli, M.; Melillo, M.; Guzzetti, F.; Rossi, M.; Palazzi, E.; von Hardenberg, J.; Brunetti, M.T.; Peruccacci, S. Implications of climate change on landslide hazard in Central Italy. *Sci. Total Environ.* **2018**, *630*, 1528–1543. [CrossRef] [PubMed]
24. Chang, K.-T.; Chiang, S.-H. An integrated model for predicting rainfall-induced landslides. *Geomorphology* **2009**, *105*, 366–373. [CrossRef]
25. Guo, X.; Cui, P.; Li, Y.; Ma, L.; Ge, Y.; Mahoney, W.B. Intensity–duration threshold of rainfall-triggered debris flows in the Wenchuan Earthquake affected area, China. *Geomorphology* **2016**, *253*, 208–216. [CrossRef]
26. Chien-Yuan, C.; Tien-Chien, C.; Fan-Chieh, Y.; Wen-Hui, Y.; Chun-Chieh, T. Rainfall duration and debris-flow initiated studies for real-time monitoring. *Environ. Geol.* **2005**, *47*, 715–724. [CrossRef]

27. Guzzetti, F.; Peruccacci, S.; Rossi, M.; Stark, C.P. Rainfall thresholds for the initiation of landslides in central and southern Europe. *Meteorol. Atmos. Phys.* **2007**, *98*, 239–267. [CrossRef]
28. Vessia, G.; Parise, M.; Brunetti, M.T.; Peruccacci, S.; Rossi, M.; Vennari, C.; Guzzetti, F. Automated reconstruction of rainfall events responsible for shallow landslides. *Nat. Hazards Earth Syst. Sci.* **2014**, *14*, 2399–2408. [CrossRef]
29. Glade, T.; Crozier, M.; Smith, P. Applying Probability Determination to Refine Landslide-triggering Rainfall Thresholds Using an Empirical "Antecedent Daily Rainfall Model". *Pure Appl. Geophys.* **2020**, *157*, 1059–1079. [CrossRef]
30. Mathew, J.; Babu, D.G.; Kundu, S.; Kumar, K.V.; Pant, C.C. Integrating intensity–duration-based rainfall threshold and antecedent rainfall-based probability estimate towards generating early warning for rainfall-induced landslides in parts of the Garhwal Himalaya, India. *Landslides* **2013**, *11*, 575–588. [CrossRef]
31. Sengupta, A.; Gupta, S.; Anbarasu, K. Rainfall thresholds for the initiation of landslide at Lanta Khola in north Sikkim, India. *Nat. Hazards* **2010**, *52*, 31–42. [CrossRef]
32. Jemec, M.; Komac, M. Rainfall patterns for shallow landsliding in perialpine Slovenia. *Nat. Hazards* **2011**, *67*, 1011–1023. [CrossRef]
33. Milne, F.D.; Brown, M.J.; Knappett, J.A.; Davies, M.C.R. Centrifuge modelling of hillslope debris flow initiation. *Catena* **2012**, *92*, 162–171. [CrossRef]
34. Amiri, M.A.; Conoscenti, C. Landslide susceptibility mapping using precipitation data, Mazandaran Province, north of Iran. *Nat. Hazards* **2017**, *89*, 255–273. [CrossRef]
35. Khan, S.; Kirschbaum, D.B.; Stanley, T. Investigating the potential of a global precipitation forecast to inform landslide prediction. *Weather Clim. Extreme* **2021**, *33*, 100364. [CrossRef]
36. Beck, H.E.; Zimmermann, N.E.; McVicar, T.R.; Vergopolan, N.; Berg, A.; Wood, E.F. Present and future Koppen-Geiger climate classification maps at 1-km resolution. *Sci. Data* **2018**, *5*, 180214. [CrossRef]
37. Iadanza, C.; Trigila, A.; Napolitano, F. Identification and characterization of rainfall events responsible for triggering of debris flows and shallow landslides. *J. Hydrol.* **2016**, *541*, 230–245. [CrossRef]
38. Sun, D.; Wen, H.; Wang, D.; Xu, J. A random forest model of landslide susceptibility mapping based on hyperparameter optimization using Bayes algorithm. *Geomorphology* **2020**, *362*, 107201. [CrossRef]
39. Wang, Y.; Sun, D.; Wen, H.; Zhang, H.; Zhang, F. Comparison of Random Forest Model and Frequency Ratio Model for Landslide Susceptibility Mapping (LSM) in Yunyang County (Chongqing, China). *Int. J. Environ. Res. Public. Health* **2020**, *17*, 4206. [CrossRef]
40. Li, C.; Ma, T.; Li, W.; Zheng, A.; Zhu, X. Fractal relation of landslide frequency and rainfall. *Chin. J. Geol. Hazard Control* **2010**, *21*, 87–93.
41. Li, C.; Ma, T.; Sun, L.; Zhu, X. A New Approach to Calibrate Antecedent Precipitation for Rainfall-triggering Landslide Forecast. *Mt. Res. Dev.* **2011**, *29*, 81–86.
42. Liu, C.; Wen, M.; Tang, C. Meteorological early warning of geo-hazards in China based on raining forecast. *Reg. Geol. China* **2004**, *23*, 303–309.